npj | flexible electronics

www.nature.com/npjflexelectron

ARTICLE OPEN

Check for updates

Wearable battery-free theranostic dental patch for wireless intraoral sensing and drug delivery

Zhenghan Shi[1,3], Yanli Lu[1,3], Shuying Shen[1], Yi Xu[2], Chang Shu[2], Yue Wu[1], Jingjiang Lv[1], Xin Li[1], Zupeng Yan[1], Zijian An[1], Chaobo Dai[1], Lingkai Su[2], Fenni Zhang[1] and Qingjun Liu[1]✉

Dental caries caused by oral microbiome dysbiosis with the elevation of acidogenic bacteria is the most prevalent non-communicable disease worldwide. Early prevention and timely fluoride treatment are crucial for caries lesion management. Herein, to address the challenges of in situ sensing and topical drug delivery within the oral cavity, a miniaturized, battery-free, and wearable dental patch system was developed for microenvironment monitoring and controlled fluoride treatment. With the integration of near-field communication, the dental patch realizes wireless energy harvesting and data transmission with mobile terminals like smartphones when attached conformally to the tooth surface. The acidic microenvironment caused by bacterial metabolism are electrochemically detected, while fluorides can be delivered locally from the electric-responsive drug delivery electrode for on-demand treatment. As flexible electronics armed to the teeth, this intraoral theranostic wearable system provides an inspiring platform for point-of-care monitoring and treatment of dental caries and oral diseases.

npj Flexible Electronics (2022)6:49 ; https://doi.org/10.1038/s41528-022-00185-5

INTRODUCTION

Microbiome colonizing different parts of the body is closely related to health, whose metabolism interacts with the host dynamically through the microenvironment[1]. The oral microbiome is one of the largest microbial communities in the body, which can lead to oral or systemic diseases when dysbiosis occurs[2]. Dental caries is the most prevalent non-communicable disease worldwide caused by the elevation of the cariogenic microbiome in the oral cavity. It is estimated that caries in permanent teeth affects 2.3 billion people, with a global prevalence of 35% for all ages[3,4]. Despite dental caries being acknowledged as a global public health challenge, it is still neglected in personal oral health management. It is often hidden and doesn't cause pain or discomfort during the disease progression. The perceptible severe toothache only occurs when the caries spreads to involve the dental pulp, which can lead to infection, sepsis, and even tooth loss[5]. Such permanent damages to the teeth require treatments including the removal of the diseased teeth tissue and the placement of the filling. In contrast, the lesion at an early stage can be easily arrested and reversed with topical fluorides exposure. Unfortunately, surgical interventions after the cavity formation remain the major clinical strategy for caries management, since the early changes of the tooth enamel are undetectable with the traditional clinical visual inspection and dental radiograph[6]. Therefore, developing a point-of-care sensing system with high sensitivity integrated with therapy is highly desired for early prevention and timely treatment of dental caries.

Caries lesion is induced by the topical dysbiosis of the oral microbiome on the tooth surface. The acidogenic and aciduric bacteria accumulate in the microenvironment and digest fermentable carbohydrates into acidic metabolites, which partially demineralize the tooth enamel over time[7,8]. The caries activity test has been developed for the clinical evaluation of the acidogenic capability of the microbiome sampled from tooth by in vitro culturing[9], yet it is time-consuming and fails to provide information on real-time oral conditions. The in situ monitoring of the topical microenvironment on the tooth surface is desired for the indication of the dynamic process of demineralization which is invisible from view. Recently, the booming flexible electronics has greatly promoted the development of wearable devices[10–13]. Integrated with electrochemical sensors, they have been applied for the continuous analysis of metabolic molecules in biofluids, which offer promising opportunities for the monitoring of the oral microenvironment fluctuations. Attempts have been made for the intraoral wearable electrochemical sensing by fixing the device onto the mouthguard[14,15]. However, the bulky system due to the rigid lithium-ion battery and data transmission module inevitably restricts the further miniaturization and flexibility of the device, which affects the wearing comfort and is unable to realize the topical oral microenvironment analysis. Alternatively, the near-field communication (NFC) technology has emerged as an energy harvesting choice for miniaturized and flexible wearable devices, allowing the transmission of data and energy simultaneously through inductive coupling[16,17]. Thus, a conformal wearable electronic system including NFC and the low-power consumption electrochemical sensor serves as an ideal solution for the in situ microenvironment monitoring in the oral cavity.

Timely treatment of the dental caries is as important as the diagnosis, as caries is often not self-limiting and can progress until the tooth is destroyed without the proper care[6]. The early-stage caries lesion can be stopped by the redeposition of minerals. Exposure to fluorides is one of the most effective measures to prevent dental caries. It can not only promote tooth remineralization together with calcium and phosphate but also inhibit the growth of caries-related bacteria[18]. Nevertheless, topical drug delivery in the oral cavity is challenging with the interferences of saliva and poor local retention[19]. Traditionally, the fluorides are delivered with toothpaste or mouthwash. Although they contain

[1]Biosensor National Special Laboratory, Key Laboratory for Biomedical Engineering of Education Ministry, Department of Biomedical Engineering, Zhejiang University, Hangzhou 310027, P. R. China. [2]Stomatology Hospital, School of Medicine, Zhejiang University, Hangzhou 310016, P. R. China. [3]These authors contributed equally: Zhenghan Shi, Yanli Lu. ✉email: qjliu@zju.edu.cn

high concentration, the utilization is poor due to the short retention time and low retention amounts. Such delivery subject to limited control may also lead to the overuse of fluorides, which can cause dental fluorosis and affect the balance of the oral microbiome[20]. Thus, a controlled topical drug delivery solution is in urgent need of oral applications. By virtue of fast response and good controllability, the electrically controlled drug release based on intrinsically conducting polymer has been developed for the feedback therapy[21]. Given the characteristic of low-power consumption, it can well match the NFC-based wearable intraoral electronic system, which provides a potential strategy for topical and on-demand fluorides delivery toward caries lesions within the oral cavity.

Herein, we report a fully integrated wearable and battery-free dental patch that can wirelessly monitor the oral microenvironment in situ and deliver drugs on demand. The dental patch consisted of the control circuit and the functional electrode array is miniaturized and flexible, which can conformally interface with the tooth. An electrochemical potentiometric sensor is developed for the detection of the topical acidic environment fluctuation caused by oral microbial metabolism on the tooth surface, thus warn about the potential caries lesions. Through electrical stimulation, fluorides are timely delivered to give feedback therapy. The NFC module is developed to achieve the wireless transmission of energy and data with mobile terminals, realizing the intraoral sensing and actively controlled drug delivery without onboard batteries. The flexible electronics armed to the teeth offer a solution for dental caries prevention, which is promising in oral disease monitoring and treatment.

RESULTS

Design of the wearable theranostic dental patch system

The oral bacteria metabolized food debris and produced acid over time on the tooth surface. The caries lesion occurred when the teeth were demineralized constantly in the acidic environment. In order to monitor the microenvironment fluctuation in situ and deliver fluorides topically in the oral cavity, a miniaturized, battery-free, and wearable dental patch system was designed for caries lesion management (Fig. 1a). Considering the wearing safety and comfort comprehensively, the dental patch was assembled in a double-layer structure to reduce the size, which consisted of a control circuit and an electrode array.

The first layer was the control circuit that enabled wireless energy harvest, sensing control, drug delivery control, and wireless data transmission. Fabricated on the polyimide (PI) substrate, the circuit was flexible and thin. For the purpose of a compact design, the circuit adopted a double-sided layout (Supplementary Fig. 1). The NFC chip, the microcontroller unit (MCU) chip, resistors, and capacitors were located on the front, while the NFC antenna made of copper wire was on the back. The second layer was the electrode array including the sensing module and the drug delivery module. The electrochemical electrodes were supported by thin and stretchable polydimethylsiloxane (PDMS) film and connected with the circuit by conductive spots. When cariogenic bacteria produced acid on the tooth, the change of pH value in the topical microenvironment would be recorded by the electrochemical potentiometric sensor of the dental patch and transmitted to the smartphone. The warnings about potential caries lesions would be given out accordingly (Supplementary Fig. 2). If necessary, the command could be sent to the drug delivery module by the customized mobile application for on-demand release of fluorides, which was an efficient way to arrest and reverse the stage of caries lesion by inhibiting bacterial activity and promoting the remineralization.

To illustrate the working principle of the dental patch system, the block diagram was shown in Fig. 1b. Through the inductive coupling under a 13.56 MHz electromagnetic field, the energy could be wirelessly transmitted from the NFC-enabled smartphone to the NFC antenna. The obtained energy was modulated by the NFC chip to a stable voltage output as the power supply for the battery-free system (Supplementary Fig. 3). In order to match the limited space in the oral cavity, the low-power MCU chip integrated with signal chain peripherals including an analog-to-digital converter (ADC), multiple operational amplifiers (Amp), and a digital-to-analog converter (DAC) was adopted to reduce the circuit size, the power consumption and the material cost (Supplementary Figs. 4, 5). For acidic microenvironment monitoring, the electrochemical open circuit potentiometry was established with the MCU chip. The potential of the pH-sensitive electrode was sampled and converted to digital signals by ADC and wirelessly transmitted to the smartphone for data processing by NFC chip and antenna. The pH value would be displayed on the screen. If it indicated that the tooth were under a long-term acidic environment, the treatment command could be given through the smartphone. For the drug delivery module, a constant potential was applied to the electrodes by DAC for the electrical release of fluorides. The release potential and time could be set on demand to adjust the amount of the fluorides delivered.

The wearable dental patch system was designed to meet the demand for in situ sensing and drug delivery within the oral cavity. As displayed in Fig. 1c I, the size, entire thickness, and total mass of the dental patch was 10 mm × 8 mm, 1.5 mm, and 90 mg, respectively. The front of the patch was the control circuit (Fig. 1c II), while the back was the electrode array (Fig. 1c III). The patch was miniaturized and lightweight (Supplementary Fig. 6). With the employment of NFC, the system not only realized the wireless communication with the mobile terminals but also got rid of the restriction of the rigid onboard batteries. The reduction of circuit components made the system more integrated, improving the comfort and safety of wearing greatly for the intraoral application. The electrochemical sensing module together with the electrically controlled drug delivery module provided an efficient theranostic platform for dental caries monitoring and treatment.

Fabrication of the flexible electrode array

To realize the real-time detection and controllable drug delivery, an electrode array based on electrochemical assays was developed for microenvironment monitoring and fluoride carrying. As illustrated in Fig. 2a, the flexible electrode array was miniaturized, ultrathin, and lightweight at 15 mg. It consisted of a multilayer stack, including the screen-printed conductive inks as the electrochemical electrode interface, copper wires and copper spots as the conductive tracks, and PI and PDMS films as the substrates and encapsulations. The two-electrode configuration was adopted for the sensing and drug delivery module, including a carbon working electrode and an Ag/AgCl reference electrode. The copper wires were fabricated by the flexible printed circuit board (FPCB) process, which were encapsulated with PI for insulation. The copper spots were designed for the circuit connection. In order to make the wearable electrode array interface on the tooth surface better, the interconnects were patterned into the serpentine shape by laser cutting technique. The array was fixed on a PDMS film with high biocompatibility, which provided a conformal attachment to the tooth. As shown in Fig. 2b, the electrode array could stand bending and stretching without mechanical fracture of the circuits (Supplementary Fig. 7). The multilayer and ultrathin design together with the serpentine tracks offered good flexibility for the electrode array and increased its tolerance to mechanical deformations, which ensured its functionality on the tooth.

The electrodes were modified layer-by-layer for sensing and drug loading (Fig. 2c). The conjugated conducting polymers like

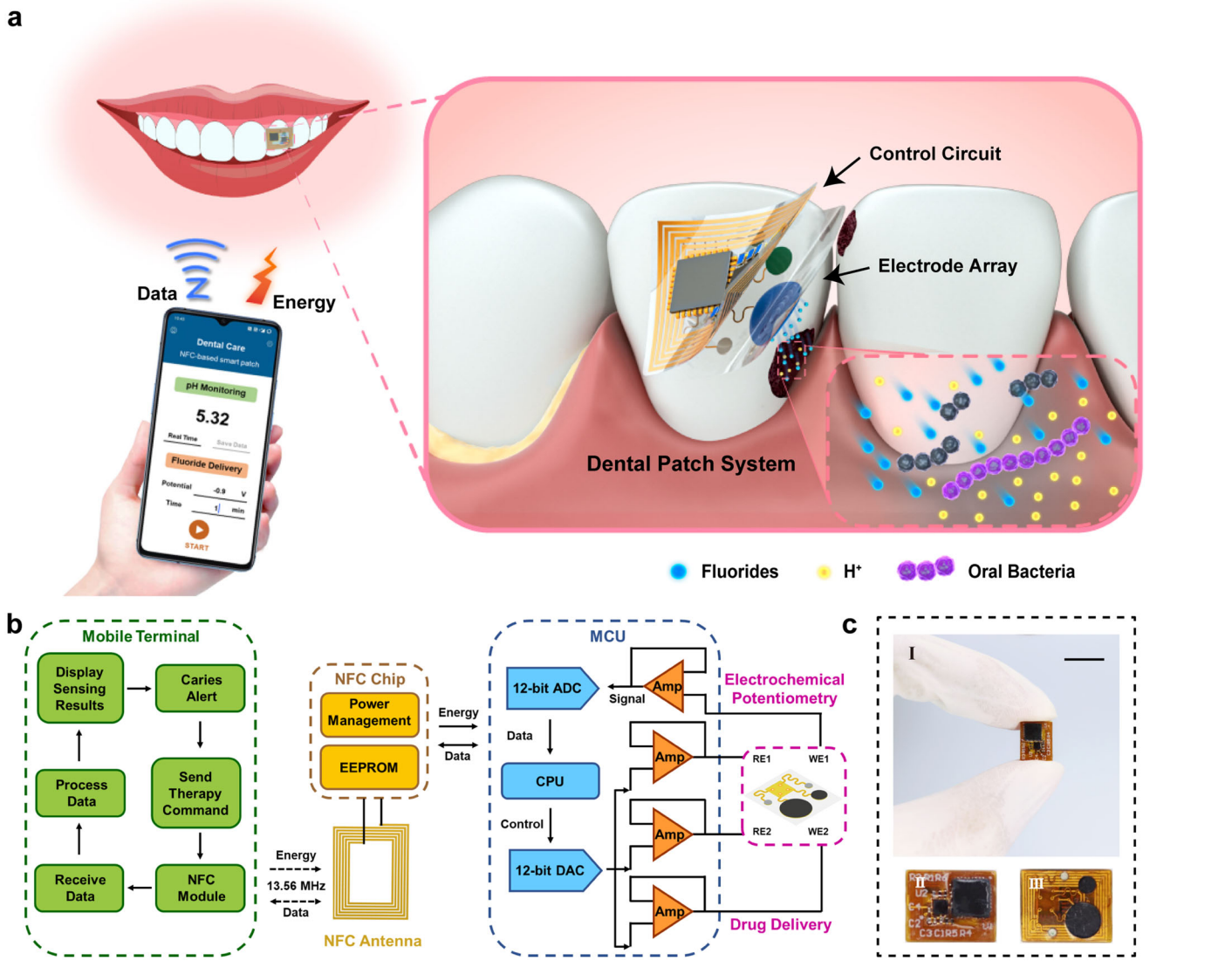

Fig. 1 The wearable theranostic dental patch system. a Schematic of the dental patch system consisting of the control circuit and the electrode array for in situ oral microenvironment monitoring and on-demand drug delivery. **b** Block diagram and working principle of the system. NFC near field communication, MCU microcontroller unit, ADC analog-to-digital converter, DAC digital-to-analog converter, CPU central processing unit, Amp operational amplifier, WE working electrode, RE reference electrode. **c** Optical image (I) of the dental patch. Scale bar, 1 cm. The front (II) was the control circuit, while the back (III) was the electrode array.

polyaniline (PANi) and polypyrrole (PPy) were ideal materials for wearable electronics due to its good stability, biocompatibility, and electrical properties[22]. For the sensor, PANi was designed as the pH sensing layer. Before the modification of the PANi, gold nanoparticles were deposited firstly on the carbon working electrode to improve the conductivity of the electrodes (Supplementary Fig. 8). PANi was then synthesized in situ on the electrode by electrochemical cyclic voltammetry (Supplementary Fig. 9). The electrode after modification was characterized by a scanning electron microscope (SEM). The PANi had a coral-like morphology (Fig. 2d), which grew on the carbon electrode modified with gold nanoparticles (Supplementary Fig. 10). The H^+ could be captured by PANi reversibly as the doping agent. With the protonation and deprotonation reaction, PANi transformed between its two states, emeraldine base and emeraldine salt, which would change the open circuit potential of the electrode[23]. The polyvinyl butyral (PVB) mixture containing carbon nanotubes and saturated sodium chloride was covered on the reference electrode to maintain a stable potential and reduce the potential drift.

For the drug delivery module, the intrinsically conducting polymer, PPy, was modified on the electrode as the electric-responsive drug carrier due to its doping and dedoping properties. When its monomer pyrrole was oxidized and polymerized to PPy, the anionic dopants in the solution would be incorporated into the main chain of the polymer to counterbalance the positive charges[24]. In order to load fluorides, the electrodes were applied with a constant current by electrochemical chronopotentiometry in the sodium fluoride solution containing pyrrole for the modification of the polypyrrole-fluoride layer (PPy/F). To reduce the spontaneous releasing of the fluorides, a polyanion, polystyrene sulfonate (PSS), was adopted as the dopant to form another polypyrrole/PSS layer (PPy/PSS) above the PPy/F layer in the same way. The anionic dopant, PSS, could form a stable combination within the main chain of the polymer, which exerted a blocking effect on the spontaneous releasing of the fluorides below[25,26]. The potential of the electrode remained steady during the synthesis, indicating the stable growth of the PPy/PSS and PPy/F (Supplementary Fig. 11). The electrode after modification

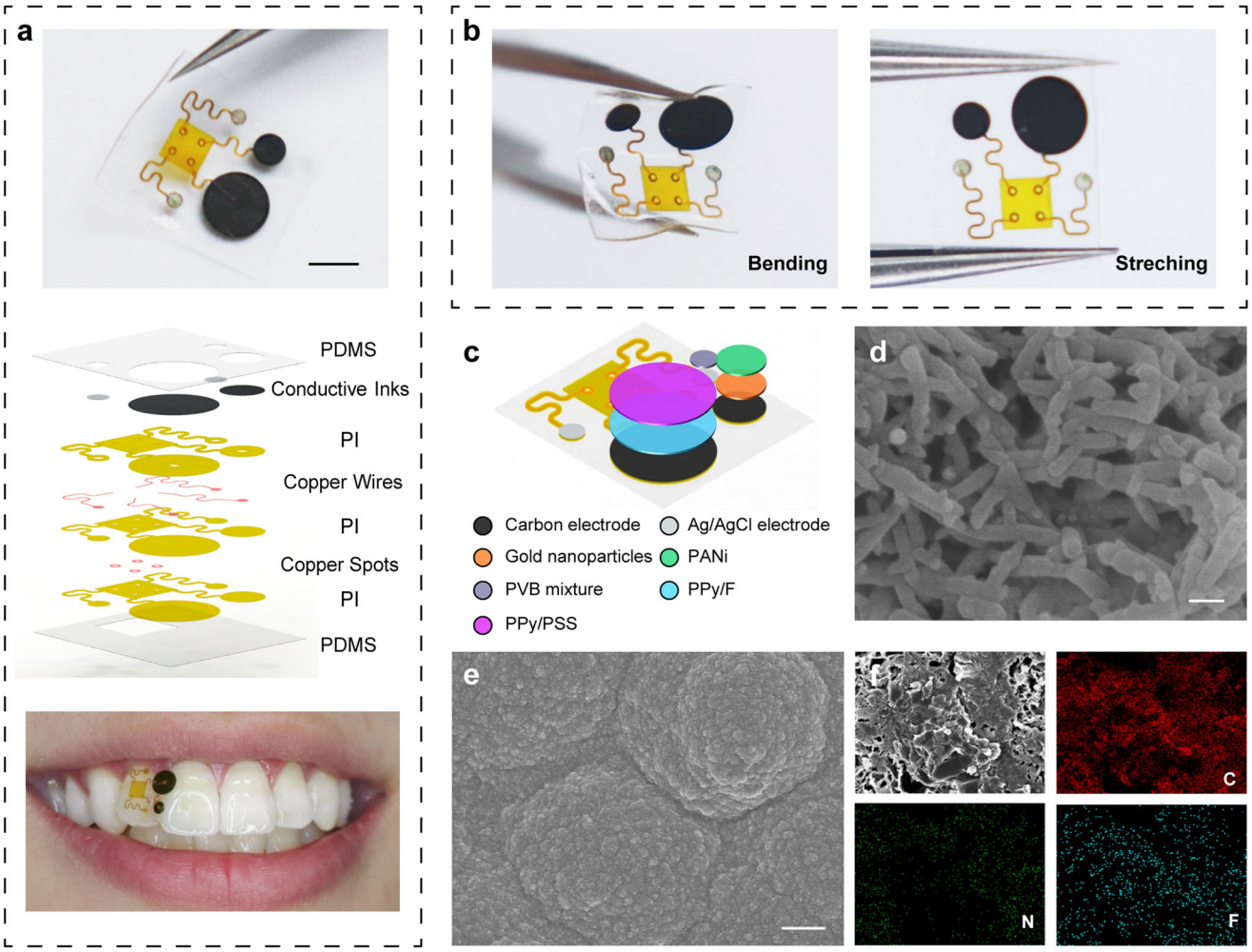

Fig. 2 Fabrication and characterization of the flexible electrode array. a Optical image and the exploded view of the electrode array. Scale bar, 3 mm. The electrode array consisted of screen-printed conductive inks as the electrochemical electrode interface, copper wires and copper spots as the conductive tracks, and PI and PDMS films as the substrates and encapsulations. The flexible electrode array was miniaturized, ultrathin, and lightweight, which could conformally interface on the tooth. **b** Mechanical deformations of the flexible electrode array including bending and stretching. **c** Schematic of multilayer modification of the electrodes in an exploded view. **d** Scanning electron microscope (SEM) image of polyaniline (PANi) modified electrode. Scale bar, 100 nm. **e** SEM image of polypyrrole (PPy) modified electrode. Scale bar, 1 μm. **f** Energy dispersive spectroscopy (EDS) images of polypyrrole/fluoride (PPy/F) electrodeposited on the working electrode of the drug delivery module, including C (red), N (green), and F (blue) elemental mapping.

was characterized by SEM. A cauliflower morphology indicated the successful preparation of PPy (Fig. 2e). The energy dispersive spectrometer (EDS) elemental analysis was used to demonstrate the composition of the drug delivery electrode. The result showed that the cauliflower structure was made up of carbon (C), nitrogen (N), and fluorine (F), which further proved that the fluorides were well doped in the PPy (Fig. 2f).

In vitro characterization and evaluation of the electrochemical sensor

In order to ensure the accuracy and reliability of the monitoring in the oral cavity, the performances of the sensor were investigated in vitro firstly. Based on the pH sensor established above, electrochemical open circuit potentiometry with a low-power consumption design was applied for sensing. The healthy oral had a pH around 7 due to the buffering function of the saliva, while the value could decrease below 5 when the caries occured[27]. To simulate the detection process of the oral microenvironment acidification when demineralization occurred, the sensor was recurrently tested in the buffer with pH changing from 8 to 3. The potential of the sensor at different pH was stable at a constant value, which showed a step response (Fig. 3a). The response of the pH sensor according to the pH changes mainly depended on the ion (H^+) exchange rate between the PANi and the solution, which occurred very rapidly (Supplementary Fig. 12). To ensure the reproducibility of the developed pH sensors, triplicate measurements were performed with different electrodes, which showed similar slopes. Although the sensitivities are close, the absolute voltage responses of the three sensors at the same pH are often different (Supplementary Fig. 13). This is because of the variations in manual preparation of the ion-selective membrane. To solve this problem, one-point calibration was used in the measuring of pH by setting the sensing potential response of pH 7 to 0 mV for each electrode. A linear relationship between the potential and the pH value was then fitted, and the coefficient of determination (R^2) was 0.9990 (Fig. 3b). The sensor showed a near-Nernstian behavior with a sensitivity of 62.97 mV per decade of H^+ concentration. The interferences of the primary electrolytes in saliva including potassium, calcium, sodium, and magnesium were also investigated at the levels of physiological concentration[28,29]. The sensor barely responded to other potential interference ions, but only showed step responses to

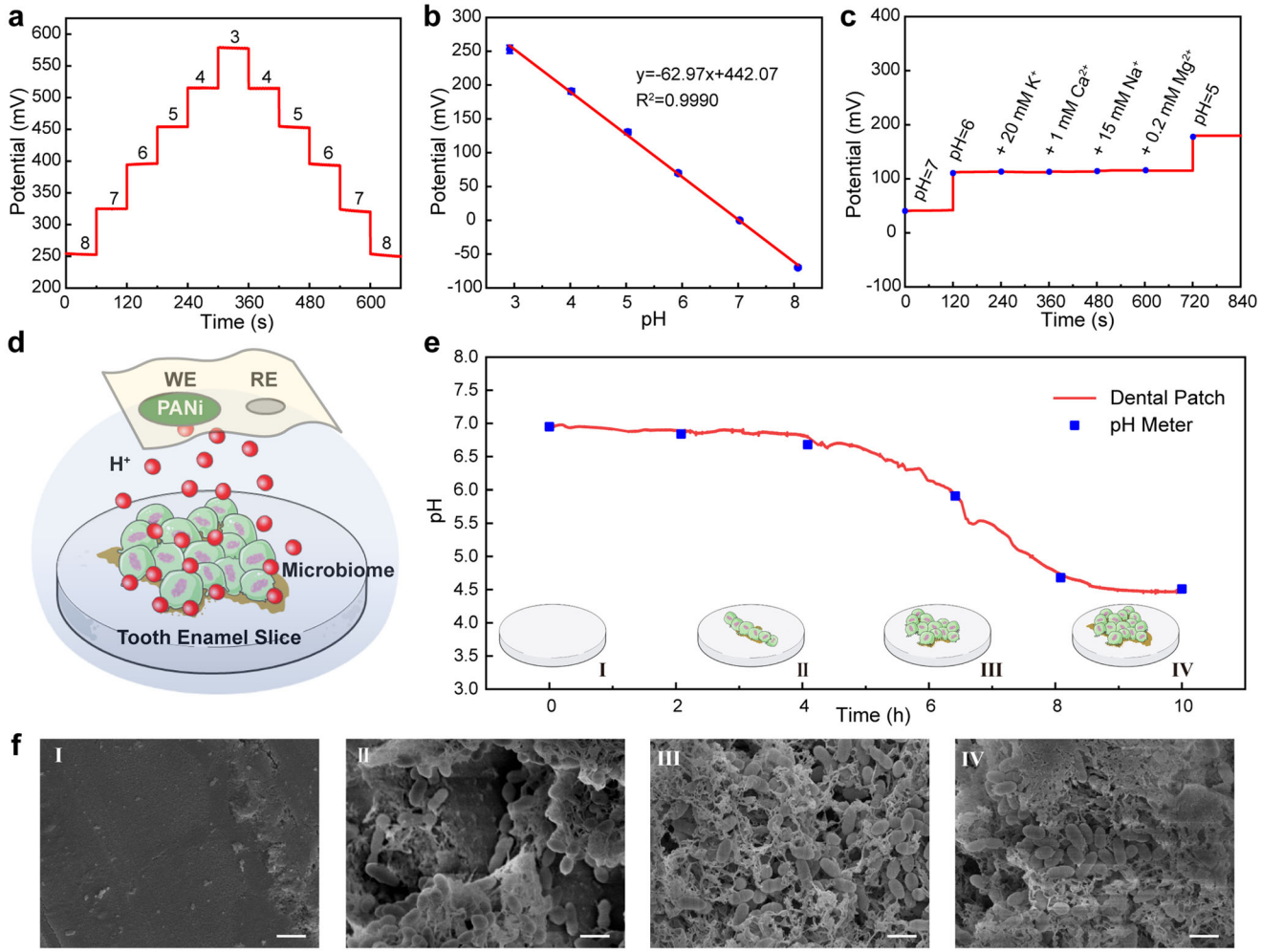

Fig. 3 In vitro evaluation of the electrochemical sensor. a Potential responses of the electrochemical sensor with the pH value changing from 8 to 3. **b** Linear fitting curve of the potential response versus pH ($N = 3$). Error bars indicated standard deviations. **c** Selectivity test of the electrochemical sensor with the interferences of K^+, Ca^{2+}, Na^+, and Mg^{2+}. **d** Schematic of the pH monitoring of *Streptococcus mutans* (*S. mutans*) dental plaque formation process. **e** The pH monitoring curve (red) of *S. mutans* dental plaque formation process, with the comparison (blue) of the standard pH meter. The insets showed the schematic of the growing process of dental plaque, including the bare tooth enamel (I), the colonization (II), proliferation (III), and mature (IV) stages of the bacteria. **f** SEM images of bare tooth enamel slices (I) and *S. mutans* dental plaque growing on the tooth enamel slices for different times, including 4 h (II), 7 h (III), and 10 h (IV). The images corresponding to the different stages of the growing process of dental plaque. Scale bars, 1 μm.

the targeted ion (H^+), which indicated that the sensor exhibited excellent selectivity (Fig. 3c).

As a chronic and progressive infectious disease mainly caused by bacterial infection, dental caries occurred under the dynamic interactions between tooth and microbiome. Among the oral microbiomes, *Streptococcus mutans* (*S. mutans*) was the most typical pathogen associated with the caries lesion[30]. Capable to produce acid and survive in a highly acidic environment, *S. mutans* was identified as the main etiological factor of dental caries[31]. Thus, the sensor was further validated by the *S. mutans* dental plaque growth experiments (Fig. 3d). The teeth enamel slice was exposed to the *S. mutans* bacterial suspension, which contained the sucrose as the carbohydrate source. The pH fluctuation of the culture medium environment was monitored by the developed pH sensor for 10 hours, which were consistent with the detection results of the standard pH meter (Fig. 3e). The continuous monitoring results showed that the pH dropped from 6.9 to 4.5 over time, indicating that the bacteria produced acid constantly during the formation process of the dental plaque.

In addition, the dental plaques formed at different pH fluctuation stages on the teeth enamel slices were studied to illustrate the relationship between bacteria proliferation and acidic metabolism. The surface of the teeth enamel was smooth at the beginning, which was made of hydroxyapatite (Fig. 3f I). It could be seen in Fig. 3e that the pH decreased quite slowly and kept near 7 at the beginning due to the buffering of electrolytes in the environment. From the fourth hour, the pH began to drop, as the bacteria colonized the tooth gradually. The bacteria could secrete water-insoluble polysaccharides, which promoted them to adhere to the tooth surface (Fig. 3f II). Then, the pH decreased rapidly with the reproduction and metabolization of the bacteria. Since *S. mutans* was highly acidogenic and aciduric, it multiplied rapidly once the acidic environment was established. At the seventh hour, the pH of the microenvironment dropped to 5.5, while a bacterial matrix with a porous structure was observed on the enamel (Fig. 3f III). The porous network matrix not only increased the adhesion area of bacteria but was also beneficial for the underneath bacteria to exchange nutrients and oxygen, providing a favorable and protective growth environment[32]. Finally, the pH of the environment reached a stable value of 4.5, which could lead to the constant demineralization of the tooth and rapid caries lesion progression. A mature dental plaque

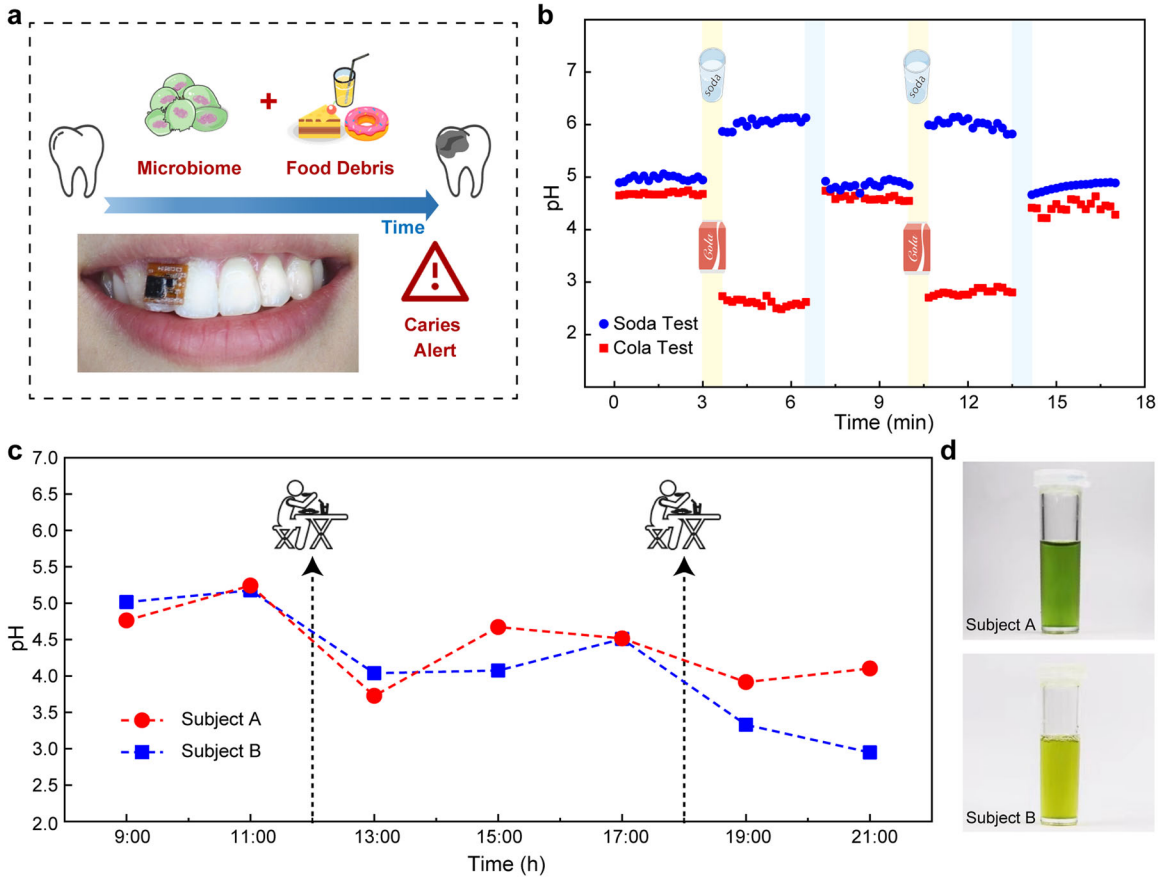

Fig. 4 In situ oral microenvironment monitoring with the dental patch. a Schematic of caries lesion detection by monitoring the topical oral microenvironment pH fluctuation. The cariogenic microbiome metabolized carbohydrates from food debris and produced acids over time, which resulted in caries lesions. The developed dental patch system could be well attached to the tooth for in situ sensing. **b** Real-time monitoring of oral pH after volunteer drank pure water (pH = 6.8), acidic cola (pH = 2.5) and alkaline soda water (pH = 8.0). The volunteer drank cola or soda water, water, cola or soda water, and water in turn. **c** Topical oral microenvironment pH fluctuation of the volunteers detected by the dental patch during a day. The volunteers had carbohydrate-rich meals at 12:00 and 18:00. **d** Caries activity of the volunteers was measured with a commercial colorimetric kit. The oral bacteria were sampled from the tooth surface and cultured for 48 h in the medium with an acid indicator. The degree of yellow indicated the capability of oral bacteria on acid production.

containing bacterial colonies and extracellular matrix came into being on the tooth enamel (Fig. 3f IV). When the bacteria was removed, the pH of the microenvironment could recover to near 7 (Supplementary Fig. 14). Above all, the developed pH sensor with high sensitivity and selectivity could monitor the acidic metabolism of the cariogenic bacteria during the formation of the dental plaque, promising to be used for the indication of the microenvironment fluctuation on the tooth enamel.

In situ oral microenvironment monitoring with the dental patch

In real-life scenarios, the main factors implicated in the dental caries process included teeth, diet, microbiome, and time[6]. The cariogenic bacteria in the microenvironment metabolized carbohydrates from food debris and produced acids over time, which caused the demineralization of tooth, thereby resulting in caries lesion. The developed smart dental patch could evaluate the acidification condition of the oral microenvironment through the real-time detection of pH fluctuation on the tooth surface, realizing the monitoring and early warning of caries lesion in progress (Fig. 4a).

The wearable dental patch could be well attached to the tooth with a transparent dental strip for in situ sensing. In order to investigate the effect of a temporary diet on the oral microenvironment, the topical pH on the tooth was recorded after the volunteer drank pure water (pH = 6.8), acidic cola (pH = 2.5), and alkaline soda water (pH = 8.0), respectively. As shown in Fig. 4b, the topical pH value increased from primary 5.0 to 6.0 after drinking the alkaline soda water and recovered after drinking the pure water. Similarly, the topical pH value decreased below 3.0 after the acidic cola consumption and recovered after drinking the water. Since the liquid beverages didn't stick to the tooth, drinking pure water could remove the remaining beverage in the oral cavity, which restored the topical oral pH to its original state. The results were in agreement with studies showing that intake of food and beverages would influence the oral pH temporarily[33], which indicated the sensor was capable of a reliable real-time intraoral pH monitoring.

To investigate the long-term oral microenvironment fluctuation affected by diet and microbial metabolism, the topical oral pH of individuals at the same site was detected by the smart dental patch per 2 h in the day (Fig. 4c). Each monitoring lasted for three minutes (Supplementary Figs. 15, 16) and the average value was taken as the detection result. The topical oral pH values of the two subjects were initially around 5.0, which remained stable without food intake in the morning. After a carbohydrate-rich meal for lunch, the pH values of them obviously decreased to 3.7 and 4.0, respectively, and had slight increases in the afternoon. After another carbohydrate-rich meal for dinner, further drops of topical oral pH were observed for both subjects. The pH value of subject B

decreased significantly from 4.5 to 3.3. At the end of the day, the pH value of subject A was higher, while the oral microenvironment of subject B showed a continuous acidification. The pH values of both subjects decreased after the meals, which was caused by the metabolism of acidogenic bacteria in the presence of fermentable food debris. The pH fluctuated between the two meals, which was due to the buffering of the saliva, as the secretion of the saliva was an important way to regulate the oral environment by the host[34].

To validate the sensing results, the caries activity of the volunteers was measured with a commercial colorimetric kit. The oral bacteria were sampled from the tooth surface and cultured for 48 h in the medium with an acid indicator. Having been widely applied to assist the clinical diagnosis of dental caries, the test was designed to detect the capability of acid production of oral bacteria, which was reflected by the yellow degree of the acid indicator[9]. As shown in Fig. 4d, the oral microbiome of subject B produced more acid than subject A after the same culturing time. The test results were consistent with the detection of the developed sensors. It indicated that subject B had higher caries activity than subject A and was more prone to suffer from dental caries. Specifically, in addition to microbial composition, the risk of caries was decided by many other factors including dietary habits, food intake, salivary buffering capacity, and genetic factors, which all had a direct influence on caries activity and varied among individuals[35]. It would be necessary to obtain the real-time oral microenvironment condition of the individual to analyze the risk of caries for the purpose of personalized dental care. Compared with the conventional time-consuming culturing assay, the smart dental patch provided an efficient and reliable solution for the evaluation of the caries activity within the oral cavity.

Early detection and monitoring of the caries lesion were greatly recommended rather than waiting until the formation of a cavity, especially for the individuals prone to dental caries[4]. When the food rich in sugar was consumed frequently or the salivary secretion was insufficient to neutralize the acids, the acidification of the oral microenvironment would be more severe and frequent, resulting in continuous demineralization of the enamel. The caries could progress rapidly without timely intervention and treatment. However, the early changes in the tooth enamel were often undetectable with the traditional clinical visual inspection. Therefore, in situ monitoring of the topical pH on the tooth surface with the smart dental patch developed in the study would be beneficial to the prevention of caries, which enables a direct real-time reflection of the enamel status. When the acidic oral microenvironment was frequently observed, an alert would be sent by the smartphone that an oral cleaning, as well as the fluorides treatment, was required.

Evaluation of the electrically controlled fluorides delivery

As fluoride exposure was one of the most effective strategies for treating early dental caries, an electrically controlled drug delivery module was integrated into the dental patch for the on-demand caries lesion treatment. Once the treatment command was given through the smartphone, the fluorides could be released locally on the tooth surface by the negative potential applied to the electrodes (Fig. 5a). When the miniaturized NFC-enabled dental patch system was placed in the NFC sensing area of the smartphone, the potential of the drug electrode rose rapidly to the set output potential and remained stable (Supplementary Fig. 17). In order to ensure the delivery performances of the module, the effects of synthesis time, natural release, and release potential were investigated. The fluorine reagents spectrophotometry assay was adopted for the determination of the fluorides. A calibration curve was established between the absorbance of the fluoride complex at 614 nm and the concentration of the fluorides, which covered the detection range from 5 to 100 μM (Fig. 5b). The fluorides were loaded on the working electrode through the polymerization of PPy. To investigate the effect of the synthesis time, the in situ polymerization and doping process of PPy/F on electrodes was performed for 5, 10, 15, and 20 min, respectively. The results showed that the amount of fluorides loaded on the electrodes increased with the synthesis time (Fig. 5c). As the most typical and common drug for dental caries prevention, fluorides could inhibit acid production by cariogenic bacteria at concentrations as low as 1 ppm[36]. The probable toxic dose which could trigger acute toxicity and require immediate treatment was defined at 5 mg/kg of body mass[37]. The long-term exposure at a dose of 5–10 mg/day could cause chronic toxicity on tooth and bone[20]. Thus, comprehensive considering the performance of the electrode, the effective fluorides amounts and the safe fluorides amounts, 20 min were taken as the polymerization time of PPy for the developed electrode in this study (Supplementary Fig. 18). Due to the diffusion effect, the fluorides doped in the PPy would release spontaneously over time. In order to enhance the control of the drug delivery, another PPy/PSS layer was covered on the PPy/F to form a bilayer structure, which was designed to reduce spontaneous releasing. As shown in Fig. 5d, the total amount of fluorides released spontaneously from the monolayered electrode (PPy/F) was 27.9 nmol in 3 h, while the amount released from the bilayered electrode was 18.4 nmol. Thus, the modification of the PPy/PSS layer could reduce the spontaneous release of fluorides.

When a potential from NFC was applied, the fluorides would dissociate from the main chain of the polymer under the electrical force, with the PPy changing from an oxidized state to a reduced state. The effect of the release potential was investigated by applying different voltages to the working electrode. Each electrical stimulation lasted for three minutes. The results showed that the amount of the fluorides delivered could be well regulated by adjusting the release potential (Fig. 5e). To evaluate the electrically controlled delivery process of the fluorides in a dynamic way, a potential of −0.9 v was applied to the electrodes periodically. The release rate under the electrical stimulation was obviously higher than the spontaneous release, which further indicated the good regulation capability of the drug delivery module on the fluorides releasing (Fig. 5f). For each stimulation period, the current was recorded, which reached about 20 μA when the fluorides were stably controlled and delivered (Supplementary Fig. 19). The power consumption of the delivery module was lower than 30 μW, which could be afforded by the miniaturized NFC-enabled dental patch system. With the advantages of good controllability and low-power consumption, the electrically controlled drug delivery based on conducting polymer would be an ideal solution for topical on-demand fluorides delivery in the oral cavity.

To evaluate the antibacterial activity of the electrically controlled fluorides delivery module, the representative cariogenic bacteria, *S. mutans*, were cultured in the medium with the fluorides delivered by the electrodes. The bacterial populations were stained by a bacterial viability kit and observed with confocal laser scanning microscopy (CLSM) (Fig. 5g). The bacteria with an intact cell membrane were stained green, while the dead or dying bacteria with a damaged membrane were stained red. The CLSM image showed that the density of the *S. mutans* populations in the treated group was lower than the control group. Besides, there were no obvious dead bacteria in the control group, while the damaged bacteria could be observed in the treated group. The effect of fluorides was related to the concentration, which would depend on the volume of the solution on the tooth surface (Supplementary Fig. 20). Fluorides could interfere with the metabolism of caries-related bacteria, thus inhibiting acid production and maintaining or even restoring the pH of the microenvironment (Supplementary Fig. 21). The results demonstrated that the system could inhibit the growth of caries-related

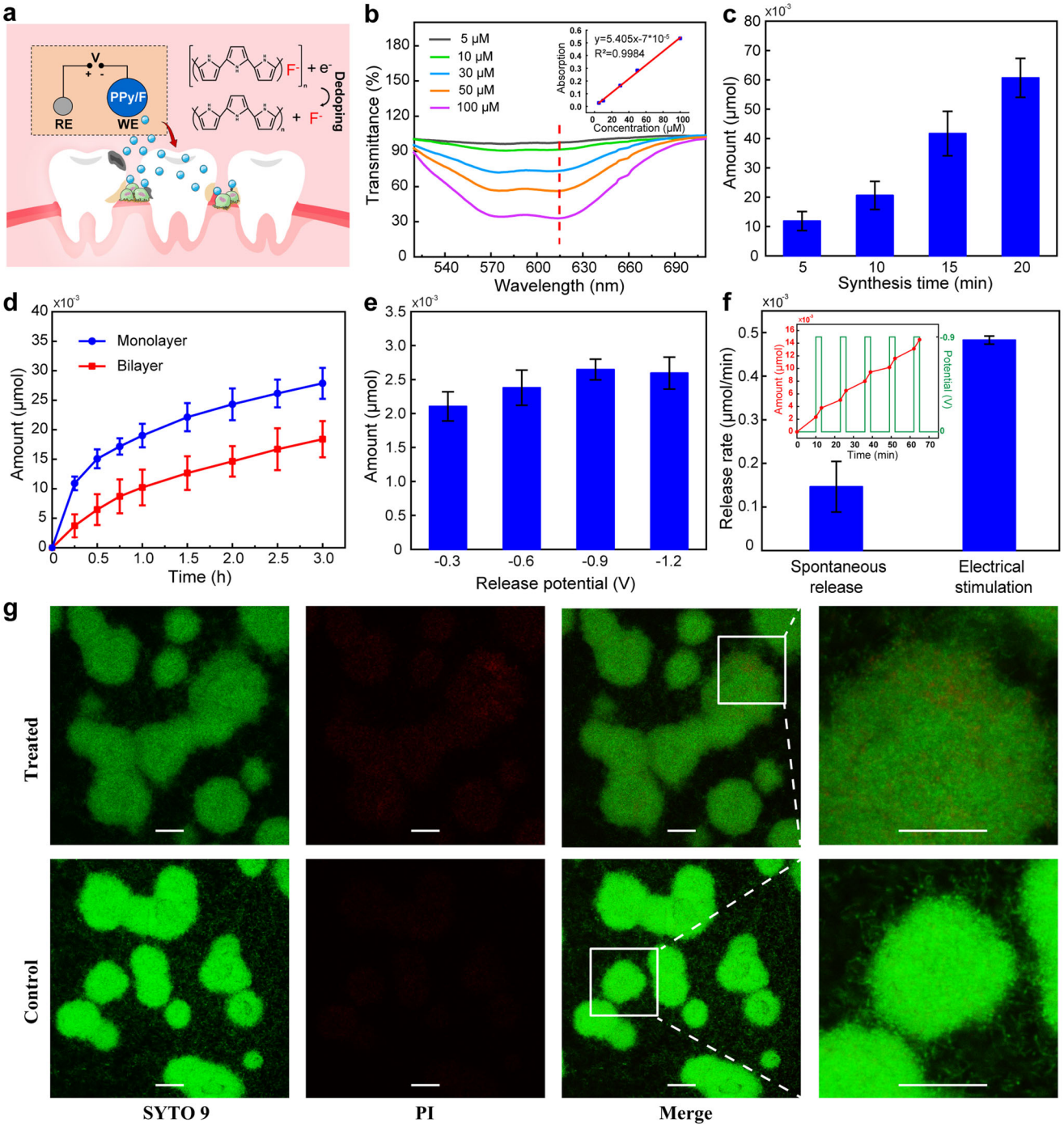

Fig. 5 Evaluation of the electrically controlled fluorides delivery. a Schematic of electrically controlled release of fluorides from the drug delivery module. Once the treatment command was given, the fluorides could be released locally on the tooth surface by the negative potential applied to the electrodes. **b** Transmission spectra of the fluoride complex with the fluorides varying from 5 to 100 μM. The inset was the calibration curve between the absorbance of the fluoride complex at 614 nm and the concentration of the fluorides. **c** Influence of synthesis time on the amount of fluorides loaded on the electrodes. **d** Amount of fluorides released spontaneously from different electrodes, including monolayer-electrode (modified with only PPy/F) and bilayer-electrode (modified with both PPy/PSS and PPy/F). **e** Effect of release potential on the amount of fluorides released from the electrodes. **f** Release rate comparison between the spontaneous release and the electrical stimulation. The release rate was defined as the amounts of fluorides released per minute from the drug delivery electrode under the spontaneous release or under the electrical stimulation. The inset was the real-time release amounts of the fluorides under the alternating action of the spontaneous release and the electrical stimulation (red). The electrical stimulation was a constant potential of −0.9 V (green). **g** Confocal laser scanning microscopy (CLSM) images of *S. mutans* samples stained by the bacterial viability kit for evaluation of the antibacterial activity of the drug delivery module. The bacteria with an intact cell membrane were stained green by the SYTO 9 nucleic acid stain, while the dead or dying bacteria with a damaged membrane were stained red by the propidium iodide (PI) nucleic acid stain. The merge referred to the overlap of two fluorescent images. Scale bars, 20 μm. Error bars indicated standard deviations.

bacteria. Furthermore, fluorides had been widely proved to be efficient in arresting and reversing the stage of caries[38,39]. Acting as the catalyst, fluorides assisted with the redeposition of calcium and phosphate into the tooth. Consequently, the developed drug delivery module could release fluorides under electrical control, providing effective treatment for caries lesions. Compared with the traditional fluorides exposure through toothpaste and mouthwash, the electrically controlled fluorides delivery module offered a sustained and on-demand drug delivery approach in the oral cavity with the support of a wearable dental patch system. The topical controlled delivery based on the sensing results not only promoted the efficient utilization of the fluorides but also reduced the risk of dental fluorosis and microbial disorder caused by overuse of fluorides.

DISCUSSION

With the increasing concerns on oral health, dental caries management was shifting from reactive intervention to proactively prevention[40]. In recent years, endeavors were devoted to the design of highly sensitive sensors to meet the demands of detecting the invisible caries lesion as early as possible. In addition to the caries activity test assay mentioned above, a fluorescent mouthguard was developed to detect the release of volatile sulfur compounds from the lesion sites[41]. A color-changing dental floss was also built with biomaterial-based colorimetric sensing mixes for oral pH detection[42]. In this study, a smart wearable dental patch system was innovatively proposed for dental caries monitoring and treatment simultaneously. Since caries lesion occurred locally in the oral microenvironment on tooth enamel due to microbiome dysbiosis, the fully integrated intraoral wearable electronics was characterized as flexible, miniaturized, and lightweight, which could be attached to the tooth conformally. The system addressed the challenges of in situ sensing and delivering drugs topically within the oral cavity. Through real-time microenvironment monitoring and on-demand fluoride delivery, the dental patch could detect and treat the invisible lesion in time rather than wait until the formation of a cavity, which provided a novel strategy for clinical and family caries prevention.

Apart from the acidity fluctuation caused by acidogenic bacteria associated with dental caries, there were abundant microbiome-related biomarkers in oral microenvironments like metabolites, antibodies, and enzymes, which could provide insights into the health information from the molecular level[43,44]. The oral cavity had the second largest and most diverse microbiome after gut in the body, whose anatomy was distinctive including tooth, gingiva, tongue, palate, and buccal mucosa[2]. Different parts of the oral cavity were colonized with different microbial communities, which were crucial to oral as well as systemic health. For example, periodontitis was another common oral disease caused by microbial dysbiosis with pathogenic bacteria accumulating around the gingival sulcus[45]. Given the capability to provide in situ detection and treatment topically, the smart dental patch was expected to enlarge applications in monitoring and regulating diverse microenvironments by interfacing with different parts in the oral cavity. Owing to the design flexibility of the microcontroller, other typical electrochemical methods including cyclic voltammetry, differential pulse voltammetry and chronoamperometry could be further developed on the dental patch for real-time quantitative analysis. According to the therapeutic demands, specific drugs like antibiotics could be selectively loaded on the patch for electrically controlled topical drug delivery. As a proof-of-concept, the proposed intraoral wearable dental patch system served as an inspiring diagnostic and therapeutic mobile health platform for oral diseases, shedding light on wearable medical electronics based on microbiome metabolism monitoring toward personalized medicine.

Despite the successful realization and validation of a wearable flexible dental patch system, some issues remain to be further improved. Firstly, from the point of view of the commercial practical use, the connection between the circuit and the electrode can adopt detachable connections such as magnetic conductive connection or plug-in conductive connection instead of solid welding. Such reusable design of the circuit will effectively reduce the cost of the application. Secondly, the user comfort and safety could be further optimized by comprehensively considering the properties of the soft encapsulation materials including the biocompatibility, rigidity, permeability and reversible adhesion capability. Besides, the employment of NFC inevitably had a short communication distance, which was largely limited to the built-in NFC module of the commercial smartphone. Mobile terminal devices with larger NFC reading coil can be customized to improve practicality.

In conclusion, a wearable intraoral theranostic dental patch system was developed with an electrochemical sensor and an electrically controlled fluorides delivery module for in situ monitoring and on-demand treatment of caries lesion. The in vitro cariogenic bacterial experiments and human trials demonstrated that the sensor had high sensitivity and reliability for the real-time detection of the topical oral microenvironment fluctuation. The fluorides released under the voltage stimulation showed good antibacterial activity. Both monitoring and therapeutic modules were wirelessly controlled and powered by an NFC-enabled smartphone, enabling timely fluoride treatment based on the signals detected by the sensor. This point-of-care system provided opportunities for intraoral wearable electronics to achieve real-time monitoring of biomarkers and on-demand medication for personalized health care applications.

METHODS

Design of the battery-free and wireless flexible circuit board

The battery-free and wireless flexible circuit board was designed for electrochemical sensing and electrically controlled drug delivery. The electronic components included the NFC chip (NT3H2111, NXP Semiconductor, Netherlands), the MCU chip (MSP430FR2355, Texas Instruments, USA), resistors, and capacitors. The NFC chip and the antenna were adopted as the energy harvesting solution for the whole system. The MCU integrated with 12-bit ADC, 12-bit DAC, and Amp was coded for the realization of open circuit potentiometry for pH sensing and the voltage stimulation for drug delivery.

Fabrication, modification, and characterization of the electrode array

A copper wire encapsulated with PI was fabricated by the process of FPCB and patterned into the serpentine shape by laser cutting. The carbon conductive ink and the Ag/AgCl conductive ink (Gwent Electronic Materials Ltd., UK) were printed onto the conductive spots as working electrode and reference electrode, respectively. The electrode array was encapsulated with PDMS films. All modifications were performed with an electrochemical workstation (CHI660, CH Instruments, USA). The modifications were performed in a three-electrode configuration with a commercial Ag/AgCl reference electrode and a commercial platinum counter electrode (CH Instruments, USA).

For the pH sensor, gold nanoparticles were firstly deposited on the working electrode to improve the conductivity by chronoamperometry. The chloroauric acid solution (0.05 wt%) with sodium sulfate (0.05 M) as the supporting electrolyte was prepared. A constant potential of −0.4 V was applied on the electrodes in the solution for 100 s for the reduction and deposition of gold nanoparticles. Then, PANi was deposited as the H^+ sensing layer. The aniline (0.1 M) was dissolved in sulfuric acid solution (0.5 M), which was polymerized to PANi and electrodeposited on the working electrode by cyclic voltammetry. The scan was performed from −0.2 to 1 V at a rate of 100 mV s^{-1} for 20 segments. The reference electrode was coated with a layer of the PVB mixture. PVB (79.1 mg), sodium chloride (50 mg), multiwalled carbon nanotubes (0.2 mg) and poly (ethylene glycol)-block-poly(propylene glycol)-block-poly(ethylene glycol)

(2 mg) were added into the methanol (1 mL) and magnetically stirred overnight. The PVB mixture (3 μL) was then drop casted onto the reference electrode and dried under the room temperature.

For the drug delivery electrode, PPy/F was electrochemical polymerized and deposited on the working electrode by chronopotentiometry. A mixed solution containing pyrrole (0.2 M) and sodium fluoride (0.2 M) was prepared. A constant current density of 2 mA cm^{-2} was applied to the electrodes for 20 min. Then, PPy/PSS was modified as the cover layer in the same manner. A constant current density of 2 mA cm^{-2} was applied to the electrodes in the mixed solution containing pyrrole (0.2 M) and PSS (0.05 M) for 20 min.

The surface morphology of the electrodes was characterized by SEM (SU8010, Hitachi, Japan). The elemental composition of PPy doped with fluorides was identified by the EDS (Oxford-Inc., UK).

In vitro characterization and evaluation of the sensor

The properties of the pH sensor including sensitivity, linearity, and repeatability were characterized by the open circuit potential measurement with the fabricated circuit board. McIlvaine's buffers with pH values ranging from 3 to 8 were prepared for the characterization and calibrated with a pH meter (Mettler Toledo, USA). The selectivity of the sensor was tested with the electrochemical workstation. A mixed solution containing K^+ (20 mM), Ca^{2+} (1 mM), Na^+ (15 mM), and Mg^{2+} (0.2 mM) were prepared for the selectivity test.

The developed sensor was validated by detecting the acid-producing process of the dental plaque in vitro. The enamel slices of the caries-free human molars were polished, ultrasonically cleaned, disinfected with UV light, and placed in a six-well plate. The *S. mutans* (UA159) cultured with brain heart infusion broth (BHI, QDRS Biotec, China) was used to form the dental plaque. The bacterial concentration was adjusted to 1.0×10^9 CFU mL^{-1} with BHI containing 1% sucrose. The bacterial suspension (6 mL) was seeded into the well containing the enamel slice. The bacteria was statically incubated at 37 °C for 10 h. The pH sensor was calibrated and applied to monitor the pH fluctuation of the culture medium environment. Due to the continuous long-term testing in the incubator, the circuit board was powered by the laptop through the USB serial port. Transwell inserts were used to eliminate the long-term biofouling of the electrode. The pH values were validated by the commercial pH meter at the different stages of incubation. The enamel slices incubated in bacterial suspensions at the different stages were analyzed by SEM to characterize the plaque growth condition.

In situ oral microenvironment monitoring with the dental patch

Intraoral monitoring of the oral microenvironment was performed on consenting individuals. The research protocol was approved by the Ethics Committee of College of Biomedical Engineering & Instrument Science at Zhejiang University. Before the experiments, all materials were UV disinfected and the pH sensor was calibrated. The dental patch was attached to the tooth surface with a transparent dental strip (Whitestrips, Crest, USA) which could be worn in the wet oral microenvironment. The topical oral pH value could be monitored when the individual wasn't eating. The effect of a temporary diet on the oral microenvironment was investigated by recording the oral pH after the volunteers consumed drinks with different pH. Then, the sensor was applied to record the topical oral pH fluctuation during the day. The pH was detected by the patch per 2 h in the day. Each monitoring lasted for 3 min and the average value was taken as the detection result. To validate the sensing results, a commercial dental caries activity test kit, Cariostat (Gangda Medical, China), was used to evaluate the acidogenic capacity of volunteers' oral microbiome. The oral bacteria were sampled from the tooth surface and cultured for 48 h in the medium with an acid indicator.

Evaluation of the drug delivery module

The fluorides loaded in the drug delivery electrodes were released by the voltage stimulation. The effects of synthesis time, natural release, and release potential on the electrically controlled drug delivery module were evaluated. Fluorides were quantified by fluorine reagents spectrophotometry assay. 1,2-Dihydroxyanthraquinonyl-3-methylamine-*N*,*N*-diacetic Acid (fluorine reagents, 1 mM), acetate buffer (pH = 4.1), acetone and lanthanum nitrate (1 mM) were firstly mixed in the volume ratio of 3:1:3:3 as the chromogenic agent for fluorides. The sample, the chromogenic agent and the deionized water were then mixed in the volume ratio of 2:2:1, and incubated in dark for 30 min. The transmission spectra of the mixture were obtained for the quantification of fluorides by an ultraviolet-visible spectrometer (USB 2000+, Ocean Optics, USA). The sodium fluoride with the concentration varying from 0.005 to 0.1 mM were tested to establish the calibration curve.

The antibacterial activity of the drug delivery module was evaluated. The coverslips (8 cm in diameter) were placed in a 48-well plate after UV disinfection. The *S. mutans* bacterial suspension (1.0×10^7 CFU mL^{-1}, 400 μL) with BHI containing 1% sucrose was seeded in the well. The drug was delivered to the well under electric stimulation. After statically incubated for 24 h at 37 °C, the samples were stained by the LIVE/DEAD *Bac*Light bacterial viability kits (L7012, Thermo Fisher, USA). The fluorescence was observed by confocal laser scanning microscopy (Leica, Germany).

DATA AVAILABILITY

The data that support the finding of this study are available from the corresponding author upon reasonable request.

Received: 11 March 2022; Accepted: 3 June 2022;
Published online: 20 June 2022

REFERENCES

1. Cho, I. & Blaser, M. J. Applications of next-generation sequencing. The human microbiome: at the interface of health and disease. *Nat. Rev. Genet* **13**, 260–270 (2012).
2. Deo, P. N. & Deshmukh, R. Oral microbiome: unveiling the fundamentals. *J. Oral. Maxillofac. Pathol* **23**, 122–128 (2019).
3. James, S. L. G. et al. Global, regional, and national incidence, prevalence, and years lived with disability for 354 diseases and injuries for 195 countries and territories, 1990–2017: a systematic analysis for the global burden of disease study 2017. *Lancet* **392**, 1789–1858 (2018).
4. Peres, M. A. et al. Oral diseases: a global public health challenge. *Lancet* **394**, 249–260 (2019).
5. Pitts, N. B. et al. Dental caries. *Nat. Rev. Dis. Prim.* **3**, 17030 (2017).
6. Selwitz, R. H., Ismail, A. I. & Pitts, N. B. Dental caries. *Lancet* **369**, 51–59 (2007).
7. Kim, D. et al. Spatial mapping of polymicrobial communities reveals a precise biogeography associated with human dental caries. *Proc. Natl Acad. Sci. USA* **117**, 12375–12386 (2020).
8. Lamont, R. J., Koo, H. & Hajishengallis, G. The oral microbiota: dynamic communities and host interactions. *Nat. Rev. Microbiol.* **16**, 745–759 (2018).
9. Nishimura, M., Oda, T., Kariya, N., Matsumura, S. & Shimono, T. Using a caries activity test to predict caries risk in early childhood. *J. Am. Dent. Assoc.* **139**, 63–71 (2008).
10. Gao, W. et al. Fully integrated wearable sensor arrays for multiplexed in situ perspiration analysis. *Nature* **529**, 509–514 (2016).
11. Sempionatto, J. R. et al. An epidermal patch for the simultaneous monitoring of haemodynamic and metabolic biomarkers. *Nat. Biomed. Eng.* **5**, 737–748 (2021).
12. He, X., Fan, C., Xu, T. & Zhang, X. Biospired Janus silk E-textiles with wet-thermal comfort for highly efficient biofluid monitoring. *Nano Lett.* **21**, 8880–8887 (2021).
13. Jin, X. et al. Fully integrated flexible biosensor for wearable continuous glucose monitoring. *Biosens. Bioelectron.* **196**, 113760 (2022).
14. Kim, J. et al. Wearable salivary uric acid mouthguard biosensor with integrated wireless electronics. *Biosens. Bioelectron.* **74**, 1061–1068 (2015).
15. Arakawa, T. et al. A wearable cellulose acetate-coated mouthguard biosensor for in vivo salivary glucose measurement. *Anal. Chem.* **92**, 12201–12207 (2020).
16. Parrilla, M., De & Wael, K. Wearable self-powered electrochemical devices for continuous health management. *Adv. Funct. Mater.* **31**, 2107042 (2021).
17. Xu, G. et al. Battery-free and wireless epidermal electrochemical system with all-printed stretchable electrode array for multiplexed in situ sweat analysis. *Adv. Mater. Technol.* **4**, 1800658 (2019).
18. Ullah, R. & Zafar, M. S. Oral and dental delivery of fluoride: a review. *Fluoride* **48**, 195–204 (2015).
19. Makvandi, P. et al. Drug delivery (nano)platforms for oral and dental applications: tissue regeneration, infection control, and cancer management. *Adv. Sci.* **8**, 2004014 (2021).
20. Gazzano, E. et al. Fluoride effects: the two faces of Janus. *Curr. Med Chem.* **17**, 2431–2441 (2010).
21. Puiggali-Jou, A., Del Valle, L. J. & Aleman, C. Drug delivery systems based on intrinsically conducting polymers. *J. Control Release* **309**, 244–264 (2019).

22. Zeglio, E., Rutz, A. L., Winkler, T. E., Malliaras, G. G. & Herland, A. Conjugated polymers for assessing and controlling biological functions. *Adv. Mater.* **31**, e1806712 (2019).
23. Pal, A., Nadiger, V. G., Goswami, D. & Martinez, R. V. Conformal, waterproof electronic decals for wireless monitoring of sweat and vaginal pH at the point-of-care. *Biosens. Bioelectron.* **160**, 112206 (2020).
24. Krukiewicz, K., Stokfisz, A. & Zak, J. K. Two approaches to the model drug immobilization into conjugated polymer matrix. *Mater. Sci. Eng. C. Mater. Biol. Appl.* **54**, 176–181 (2015).
25. Fonner, J. M. et al. Biocompatibility implications of polypyrrole synthesis techniques. *Biomed. Mater.* **3**, 034124 (2008).
26. Svirskis, D., Travas-Sejdic, J., Rodgers, A. & Garg, S. Electrochemically controlled drug delivery based on intrinsically conducting polymers. *J. Control Release* **146**, 6–15 (2010).
27. Bowen, W. H. The Stephan curve revisited. *Odontology* **101**, 2–8 (2013).
28. Urbanowicz, M. et al. Simultaneous determination of Na^{+}, K^{+}, Ca^{2+}, Mg^{2+} and Cl^{-} in unstimulated and stimulated human saliva using all solid state multisensor platform. *Electroanal* **29**, 2232–2238 (2017).
29. Aps, J. K. & Martens, L. C. Review: the physiology of saliva and transfer of drugs into saliva. *Forensic Sci. Int* **150**, 119–131 (2005).
30. Radaic, A. & Kapila, Y. L. The oralome and its dysbiosis: New insights into oral microbiome-host interactions. *Comput. Struct. Biotechnol. J.* **19**, 1335–1360 (2021).
31. Takahashi, N. & Nyvad, B. The role of bacteria in the caries process: ecological perspectives. *J. Dent. Res.* **90**, 294–303 (2011).
32. Klein, M. I., Hwang, G., Santos, P. H., Campanella, O. H. & Koo, H. Streptococcus mutans-derived extracellular matrix in cariogenic oral biofilms. *Front. Cell Infect. Microbiol.* **5**, 10 (2015).
33. Johansson, A. K., Lingstrom, P., Imfeld, T. & Birkhed, D. Influence of drinking method on tooth-surface pH in relation to dental erosion. *Eur. J. Oral. Sci.* **112**, 484–489 (2004).
34. Animireddy, D. et al. Evaluation of pH, buffering capacity, viscosity and flow rate levels of saliva in caries-free, minimal caries and nursing caries children: an in vivo study. *Contemp. Clin. Dent.* **5**, 324–328 (2014).
35. Rosier, B. T., Marsh, P. D. & Mira, A. Resilience of the oral microbiota in health: mechanisms that prevent dysbiosis. *J. Dent. Res.* **97**, 371–380 (2018).
36. Marquis, R. E. Diminished acid tolerance of plaque bacteria caused by fluoride. *J. Dent. Res.* **69**, 672–675 (1990).
37. Whitford, G. M. Acute and chronic fluoride toxicity. *J. Dent. Res.* **71**, 1249–1254 (1992).
38. Featherstone, J. D. B. Prevention and reversal of dental caries: role of low level fluoride. *Community Dent. Oral.* **27**, 31–40 (1999).
39. Marinho, V. C. C., Worthington, H. V., Walsh, T. & Clarkson, J. E. Fluoride varnishes for preventing dental caries in children and adolescents. *Cochrane Database Syst. Rev.* **7**, CD002279 (2013).
40. Watt, R. G. et al. Ending the neglect of global oral health: time for radical action. *Lancet* **394**, 261–272 (2019).
41. Li, X. et al. A transparent, wearable fluorescent mouthguard for high-sensitive visualization and accurate localization of hidden dental lesion sites. *Adv. Mater.* **32**, e2000060 (2020).
42. Matzeu, G. et al. Functionalized mouth-conformable interfaces for pH evaluation of the oral cavity. *Adv. Sci.* **8**, e2003416 (2021).
43. Zheng, X. et al. Smart biosensors and intelligent devices for salivary biomarker detection. *Trend Anal. Chem.* **140**, 116281 (2021).
44. Fuentes-Chust, C. et al. The microbiome meets nanotechnology: opportunities and challenges in developing new diagnostic devices. *Adv. Mater.* **33**, e2006104 (2021).
45. Curtis, M. A., Diaz, P. I. & Van Dyke, T. E. The role of the microbiota in periodontal disease. *Periodontol 2000* **83**, 14–25 (2020).

ACKNOWLEDGEMENTS

This work was supported by the National Natural Science Foundation of China (Grant No. 81971703, 81801793), and the National Key Research and Development Program (Grant No. 2018YFC1707701).

AUTHOR CONTRIBUTIONS

Z.S. and Y.L. contributed equally to this work. Z.S., Y.L., and Q.L. conceived the project. Z.S., S.S., Y.X., C.S., Y.W., J.L., X.L., Z.Y., Z.A., and C.D. performed the experiments. Z.S., Y.L., S.S., L.S., and F.Z. analyzed the data. Z.S., Y.L., and Q.L. wrote, reviewed, and edited the paper. All the authors designed the experiments and contributed to discussing and commenting on the manuscript.

COMPETING INTERESTS

The authors declare no competing interests.

ADDITIONAL INFORMATION

Supplementary information The online version contains supplementary material available at https://doi.org/10.1038/s41528-022-00185-5.

Correspondence and requests for materials should be addressed to Qingjun Liu.

Reprints and permission information is available at http://www.nature.com/reprints

Publisher's note Springer Nature remains neutral with regard to jurisdictional claims in published maps and institutional affiliations.